NJC

PAPER

View Article Online
View Journal | View Issue

Cite this: *New J. Chem.*, 2014, **38**, 1694

Experimental and computational studies of borohydride catalyzed hydrosilylation of a variety of C═O and C═N functionalities including esters, amides and heteroarenes†

Michael G. Manas,‡[a] Liam S. Sharninghausen,‡[a] David Balcells*[b] and Robert H. Crabtree*[a]

Received (in Porto Alegre, Brazil) 26th November 2013,
Accepted 13th February 2014

DOI: 10.1039/c3nj01485a

www.rsc.org/njc

Sodium borohydride and a series of related borohydrides catalyze a transition metal-free hydrosilylation of a variety of C═O and C═N functionalities under mild conditions. Importantly, many of these reactions are possible using the cheap and environmentally benign hydrosilane polymethylhydrosiloxane. A mechanism is proposed based on experimental and computational results.

1. Introduction

The catalytic hydrosilylation of carbon–heteroatom multiple bonds is of continuing interest and has become a popular topic in the recent literature.[1–5] Hydrosilylation of carbonyls and imines generally produces the corresponding silyl ethers and silyl amines that are easily converted to alcohols or amines through acidic cleavage. This provides an alternative to the well-established stoichiometric reduction using metal-hydride or borohydride reagents.[6] The mild and selective nature of the reaction, as well as the easy availability of inexpensive and environmentally benign hydrosilanes, such as polymethylhydrosiloxane (PMHS), provides a useful procedure for these reductions.[1] Hydrosilylation has another potential advantage in allowing isolation of the silylated intermediates that can act as protected alcohols or amines.

A wide variety of transition metal hydrosilylation catalysts have been shown to mediate reduction of C═C, C═O and C═N bonds,[1–5,7,8] but metal-free hydrosilylation is an attractive and effective alternative.[7] Most of the known transition metal-free catalysts operate either through Lewis base or Lewis acid activation of the hydrosilane. Nucleophilic catalysts such as CsF[9] or TBAF[10–12] are thought to form reactive, pentacoordinate Si intermediates capable of hydride donation to the substrate. Lewis acid catalysts such as $B(C_6F_5)_3$ form a three center–two electron bond between the silyl-hydride and the Lewis acidic center, facilitating attack at silicon by a C═O oxygen[13–15] followed by hydride attack at the carbonyl carbon by a borohydride intermediate.[16] Although transition metal-free catalysis has been seen for hydrosilylation of a range of substrates[7] including aldehydes and ketones,[9,14] esters,[11,14] amides,[12,17] imines[18,19] and nitriles,[12] as well as ether cleavage,[20] there is room for improvement in terms of substrate scope, catalyst loading and cost of both catalyst and silane.

We now find that a catalytic amount of a borohydride brings about hydrosilylation of aldehydes, ketones, esters, amides, imines, and N-heterocycles under mild conditions. In comparison to these borohydrides, previously reported Lewis acid borane catalysts are either expensive, as for $B(C_6F_5)_3$, or difficult to handle, as for BF_3.[13,14] Of the borohydride catalysts screened in this study, lithium triethylborohydride has the broadest substrate scope, while sodium borohydride is notable for its low cost and ease of use. Importantly, most of the $LiHBEt_3$-catalyzed transformations described here can be achieved with PMHS, a cheap and environmentally benign hydrosilane polymer, as reductant. We therefore have a simple hydrosilylation procedure, using a commercially available hydride catalyst and cheap reagents under mild conditions. Mechanistic studies were undertaken in order to understand this unusual reaction.

2. Results and discussion

2.1 Catalytic screening

These studies began as an effort to develop first row transition metal hydrosilylation catalysts, of which relatively few are known. In control reactions, we found clean and efficient conversion of benzaldehyde to the benzylsilyl ether without the ostensible Ni catalyst. With 1 equivalent of $SiPhH_3$, 5 mol% of $LiHBEt_3$ was an

[a] *Department of Chemistry, Yale University, P.O. Box 208107, New Haven, CT 06520-8107, USA. E-mail: robert.crabtree@yale.edu*
[b] *Centre of Excellence for Theoretical and Computational Chemistry (CTCC), Dept. of Chemistry, University of Oslo, Oslo, 0315 Norway. E-mail: david.balcells@kjemi.uio.no*

† Electronic supplementary information (ESI) available. See DOI: 10.1039/c3nj01485a

‡ These authors contributed equally to this research.

effective catalyst in THF at 20 °C over 1 hour. The following discussion therefore refers to the transition metal-free system. The hydrosilylation of various carbonyl substrates was catalyzed by 5 mol% $LiHBEt_3$ with $SiPhH_3$ or PMHS in THF under inert atmosphere (eqn (1) and (2)). The resulting silyl ethers were cleaved by basic work-up to form the respective alcohols. For aldehydes and ketones (Table 1, entries 1–4), the reaction proceeds to completion in 1 hour with a ~35 mol% loading of $SiPhH_3$ with respect to carbonyl substrate, indicating that the silane is able to deliver all three of its hydride equivalents.

The silyl ether intermediates were identified in GC-MS spectra of the crude reaction mixture. Trisubstituted $SiPh(OR)_3$ was the major product while disubstituted $SiPhH(OR)_2$ was a minor product (see ESI,† page S6). Similar yields were obtained for hydrosilylation of carbonyl substrates with PMHS as silane (Table 1, entries 1, 3, 4, 6 and 8). Diphenyl- and triphenylsilane in the appropriate stoichiometric ratios were not as reactive as $SiPhH_3$ (see ESI,† Table S1). As the yields with diphenyl- and triphenylsilane were lower than with the generally less reactive PMHS it is possible that this lower activity can be attributed to steric effects. Extension to reduction of esters and tertiary amides proved possible by heating to 60° and using 1.05 equivalents of $SiPhH_3$ or three equivalents Si–H in PMHS (Table 1, entries 6–9). ^{1}H NMR analysis showed that, prior to work-up or cleavage, tertiary amide hydrosilylation directly yields the tertiary amine as well as a mixture of siloxanes (eqn (2)). Successful amide and ester reduction is notable as this is a much more difficult reaction. The silylation of both cinnamaldehyde and ethylcinnamate with excess silane at 60° selectively yields cinnamyl alcohol with no trace of the fully reduced 3-phenyl-1-propanol (Table 1, entries 5 and 7). Our system therefore selectively reduces α,β-unsaturated carbonyls to the unsaturated silyl-ethers, a desirable selectivity pattern.

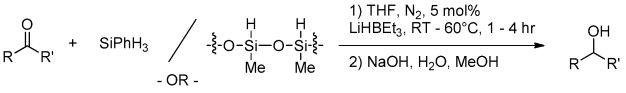

(1)

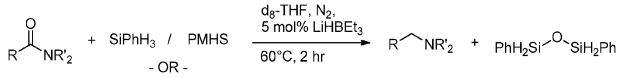

(2)

Table 1 Hydrosilylation of carbonyl groups catalyzed by $LiHBEt_3$

Entry	Substrate	Product	Silane (equiv.)	Time (h)	Temp. (°C)	Yield[c] (%)
1	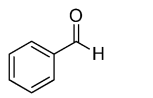	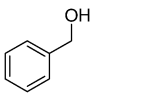	0.35[a] 1.5[b]	1	RT	>95[a] >95[b]
2	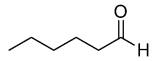	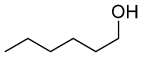	0.35[a]	1	RT	>95[a]
3	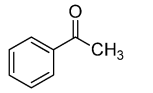	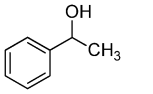	0.35[a] 1.5[b]	1	RT	>95[a] >95[b]
4	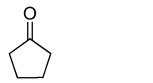	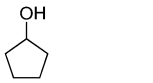	0.35[a] 1.5[b]	1	RT	>95[a] 80[b]
5	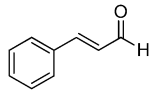	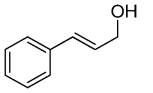	1.05[a]	4	60	93[a]
6	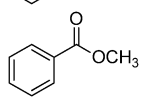	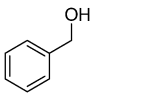	1.05[a] 3.0[b]	4	60	>95[a] >95[b]
7	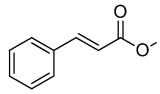	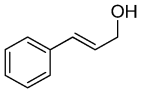	1.05[a]	4	60	>95[a]
8	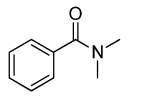	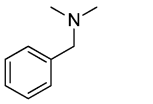	1.05[a] 3.0[b]	2	60	>95[a] 82[b]
9	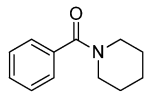	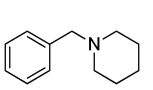	1.05[a]	2	60	94[a]

Experiments run with $LiHBEt_3$ 1 M in THF (0.06 mmol, 5 mol%), carbonyl substrate (1.20 mmol) in THF (4 ml) under 1 atm N_2 at RT or 60 degrees. [a] $SiPhH_3$ (0.42 mmol, 0.35 equivalents–1.26 mmol, 1.05 equivalents) used as silane. [b] Polymethylhydrosiloxane (0.108 ml, 1.5 equivalents Si–H or 0.216 ml, 3.0 equivalents Si–H) used as silane. [c] Yield determined by ^{1}H NMR spectroscopy using 1,3,5-trimethoxybenzene as an internal standard.

The $LiHBEt_3$ system is also active in the hydrosilylation of N-heterocycles and imines, reactions for which there are few prior examples either with[2,21,22] or without[23] a transition metal. We find that 5 mol% of $LiHBEt_3$ catalyzes the hydrosilylation of a range of heterocycles at 60° in 6–36 h (eqn (3); Table 2, entries 1–7). Quinolines and quinoxaline yield tetrahydro-products, together with <7% of the 1,2- and 1,4-dihydro-products. Reduction of 1,10-phenanthroline gives 1,2,3,4,7,8,9,10-octahydro- and 1,2,3,4-tetrahydro-products without forming any dihydro-, hexahydro-, or other species (Table 2, entry 7). Acridine (Table 2, entry 6) is converted to the 1,4-dihydro species, consistent with a 1,4 addition. Transition metal catalyzed hydrogenation of heterocycles often proceeds *via* initial 1,4 hydrogenation followed by a 1,3 hydride shift to give an easily reduced imine.[24] A similar mechanism for hydrosilylation seems less feasible owing to the difficulty of a 1,3 silane shift,[23] but the alternative would require H–Si addition across a C=C bond which we have not seen in any other substrate. Imine reduction requires 2 hours at 45° with 0.35 equiv. of $SiPhH_3$, affording near-quantitative yields of the respective amines after basic work-up (Table 2, entries 8 and 9). Selected heterocycle and imine substrates were also reduced using PMHS in generally lower but still useful yields (Table 2, entries 2, 5 and 8).

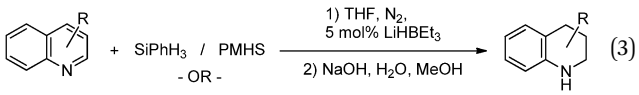

(3)

Both $LiBH_4$ and $NaBH_4$ are less active catalysts for hydrosilylation under similar conditions but they have the advantage that the reactions proceed without exclusion of air. $NaBH_4$ proved to be a more effective catalyst than the Li or K salts (see ESI,† Table S2, entries 1–3). The Li salt is highly

Table 2 Hydrosilylation of heterocycles and imines catalyzed by $LiHBEt_3$

Entry	Substrate	Product	Silane (equiv.)	Time (h)	Temp. (°C)	Yield[d] (%)
1	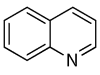	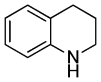	1.05[a]	24	60	71[a,c]
2	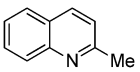	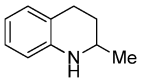	1.05[a] 3.0[b]	24	60	75[a] 50[b]
3	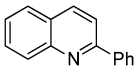	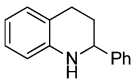	1.05[a]	24	60	52[a]
4	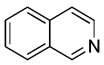	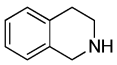	1.05[a]	24	60	69[a]
5	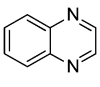	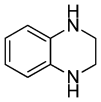	1.05[a] 3.0[b]	6[a] 24[b]	60	90[a] 55[b]
6	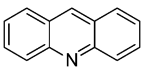	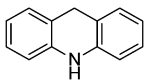	0.70[a]	24	60	>95[a]
7	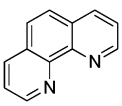	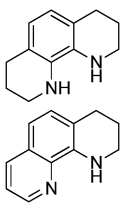	2.10[a]	36	60	55[a] 26[a]
8	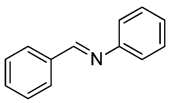	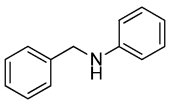	0.35[a] 1.5[b]	2[a] 4[b]	45	>95[a] 85[b]
9	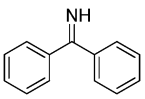	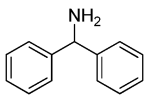	0.35[a]	2	45	>95[a]

Experiments run with $LiHBEt_3$ 1 M in THF (0.066 mmol, 5 mol%) and substrate (1.32 mmol) in THF (4 ml) at 60 degrees under 1 atm N_2. [a] $SiPhH_3$ (0.46 mmol, 0.35 equivalents to 2.772 mmol, 2.10 equivalents) used as silane source. [b] Polymethylhydrosiloxane (0.119 ml, 1.5 equivalents Si–H or 0.238 ml, 3.0 equivalents Si–H) used as silane source. [c] <7% of dihydro-products also observed. [d] Yield determined by ^1H NMR spectroscopy using 1,3,5-trimethoxybenzene as an internal standard.

Table 3 Hydrosilylation of aldehydes and ketones catalyzed by $NaBH_4$

Entry	Catalyst loading	Substrate	Time (h)	Yield[c] (%)
1	5 mol%	Benzaldehyde	1	>95
2	2 mol%	Benzaldehyde	1	92
3	Sat'd sol'n	Benzaldehyde'	1	89
4	5 mol%	4-Nitrobenzaldehyde	1	>95
5	5 mol%	4-Chlorobenzaldehyde	1	>95
6	5 mol%	4-*tert*butylbenzaldehyde	1	>95
7	5 mol%	4-Methoxybenzaldehyde	1	>95
8	5 mol%	Hexanal	1	>95
9	5 mol%	Cinnamaldehyde	1	48
10	5 mol%	Acetophenone	2/2[a,b]/24[b]	30/>95/>95
11	5 mol%	4-Methoxyacetophenone	2	10
12	5 mol%	4-Chloroacetophenone	2	76
13	5 mol%	4-Nitroacetophenone	2	80
14	5 mol%	Cyclopentanone	2[a,b]/24[b]	70/65
15	5 mol%	Benzophenone	2[a,b]/24[b]	81/>95
16[d]	5 mol%	Benzaldehyde	2[a,b]/20[a,b]	46/>95
17[d]	5 mol%	Acetophenone	2[a,b]/20[a,b]	28/>95
18[d]	5 mol%	Cyclopentanone	2[a,b]/20[a,b]	44/57

Experiments run with $NaBH_4$ (0.052 or 0.13 mmol), substrate (2.64 mmol) $SiPhH_3$ (0.881 mmol, 0.35 equivalents), entries 1–15, or polymethylhydrosiloxane (0.216 ml, 1.5 equivalents Si–H) entries 16–18 in THF (4 ml) at RT or 45 degrees. [a] Reactions run at 45 °C. [b] Reactions run under 1 atm N_2. [c] Yield determined by ^1H NMR spectroscopy using 1,3,5-trimethoxybenzene as an internal standard. [d] Reaction run with PMHS as silane source.

hygroscopic, making it more difficult to handle than the Na or K salts; this could also explain its lower activity if some of the catalyst was degraded by ambient humidity. As a result of its ease of handling, low cost and good activity, $NaBH_4$ was selected for further study. A variety of aldehydes and ketones were screened for hydrosilylation using ~35 mol% loading of $SiPhH_3$ and variable mol% loading of borohydride in dry THF and processed with a simpler acidic work-up for more rapid screening. The $NaBH_4$-catalyzed hydrosilylation of benzylic aldehydes proceeded efficiently and tolerated a variety of substituents at the 4-position of the arene ring (Table 3, entries 4–7).

Since $NaBH_4$ was not fully dissolved in 4 ml of THF at 5 mol% loading, we compared the rate of hydrosilylation after 1 hour using 5 mol%, 2 mol% and a saturated solution[25] and found that the rates were nearly the same (Table 3, entries 1–3). This suggests that only the dissolved $NaBH_4$ is effective, in contrast to the case for some other metal-free systems.[9] Despite this, 5 mol% was kept as the catalyst loading for our work to ensure having a conveniently weighable quantity and correspondingly reproducible results. $NaBH_4$ showed activity comparable to $LiHBEt_3$ for the reduction of benzylic aldehydes, but was less efficient for the reduction of ketones (Table 3, entry 10). For comparable conversion, ketones needed either longer reaction times or slightly elevated temperatures (Table 3, entries 10–15). As expected, electron-withdrawing groups such as nitro at the 4-position accelerated the reduction of acetophenones (Table 3, entries 10–13). Esters, amides and imines gave poor yields under these mild conditions. With the milder PMHS as silane source, high yields were obtained at elevated temperatures and extended reaction times (Table 3, entries 16–18).

Thus, the combination of $NaBH_4$ and PMHS provides a cheap and benign procedure for hydrosilylation of aldehydes and ketones.

2.2 Mechanism

The mechanism was studied by a combination of experimental and computational methods. In past transition metal-free systems, a nucleophile was proposed to attack the hydrosilane to give a transient 5-coordinate, hypervalent silane species capable of hydride donation.[7,9,16] Oestereich, *et al.*,[16] showed that nucleophilic attack on Si is also the likely mode of action under $B(C_6F_5)_3$ catalysis. Piers, *et al.*,[15] also suggested that the Lewis acid acts as a hydride abstractor and forms a coordination complex between the silane and the borane. Accordingly, we propose that a nucleophile present in our system activates the silane substrate, forming a hypervalent Si intermediate that

promotes hydride transfer from Si. A Lewis acid derived from $NaBH_4$ may also play a role in stabilizing the hypervalent intermediate and encouraging hydride transfer.

One potential nucleophile that could be present under the reaction conditions of the hydrosilylation of benzaldehyde is the alkali metal alkoxide salt formed from the stoichiometric reduction of benzaldehyde with $NaBH_4$. A number of experimental results are consistent with nucleophilic attack of this alkoxide on the silane. Lithium benzyloxide was independently synthesized and isolated through stoichiometric reduction of benzaldehyde. This alkoxide salt in a 10 mol% loading could replace the $NaBH_4$ catalyst under the conditions of Table 1, entry 1. After 1 hour, the reaction gave a 26% conversion of benzaldehyde to benzyl alcohol, discounting the protonated alkoxide added as catalyst. By comparison, the same reaction carried out with the addition of 10 mol% of BH_3 gave a >95% conversion showing a great improvement over the system lacking borane. This shows that (i) alkoxide formation and subsequent attack on the silane are potential steps in the mechanism and (ii) the presence of additional Lewis acid considerably increases the rate of reaction. While this supports the potential formation of a 5-coordinate hypervalent silane intermediate, we were not able to isolate or observe any such species.

We also varied the alkali metal cation in MBH_4. KBH_4 (5 mol%) gave only poor yields of the reduced product, presumably attributable to the role of M, but addition of excess alkali metal ions gave no increase in activity. Using 5 mol% of KBH_4 in addition to 20 mol% of $NaBF_4$ or $LiBF_4$ gave nearly identical yields after 1 hour; 10% yield *versus* 11% and 9% respectively (see ESI,† Table S2, entries 8 and 9). In addition, it was found that sequestration of the alkali metal through the addition of 15-crown-5 ether to a standard hydrosilylation using 5 mol% of $NaBH_4$ gave no change in reactivity (see ESI,† Table S2, entry 10). This does not fully rule out a potential role for the sodium ions, since the sequestration by the crown ether only occurs in an equatorial belt around the cation, leaving axial sites on the cation available for coordination. However, crown ether binding would cause a steric hindrance which could reasonably affect the reaction rate if the alkali metal is an essential component of an intermediary species. Based on this evidence, we tentatively suggest that the alkali metal does not play an essential role and that the borane is the more likely active Lewis acid; the low reactivity of KBH_4 may result from poor solubility in THF.

We propose that the nucleophile in the $NaBH_4$ system is the alkoxide or amide anion formed by substrate reduction. The resulting borane may act as a Lewis acid, removing a hydride from the hypervalent intermediate to yield the silyl-ether products and regenerating the borohydride catalyst. It is unclear if the borane leaves the reaction sphere during the catalysis or if it remains associated with the nucleophile after the initial hydride donation.

Alternative mechanistic paths were considered. The exclusion of light had no effect, ruling out photochemical mechanisms. The addition of stable organic radical inhibitors such as pyrene gave no change in reactivity, supporting a nonradical mechanism (see ESI,† Table S2, entry 4).

The mechanism was further explored by computing the change in enthalpy for a series of elementary steps in the addition of $SiPhH_3$ to PhCHO (see Table 4). These ΔH values were calculated at the DFT(M06)/6-311+G** level and included the solvent effects of THF (see Computational details). The catalyst, $NaBH_4$, starts by transferring a hydride to either $SiPhH_3$ or PhCHO. Hydride transfer to PhCHO is endothermic but more favourable than hydride transfer to $SiPhH_3$, as shown by the ΔH values found for entries 2 and 3 in Table 4, 58.0 and 25.0 kcal mol^{-1}, respectively. In addition, the resulting ion pair, $PhCH_2ONa$, is largely stabilized by the addition of $SiPhH_3$, ΔH = −13.2 kcal mol^{-1} (Table 4, entry 4), which yields the formation of a Si–O bond between these two species, d(Si–O) = 1.93 Å. The resulting intermediate, $PhCH_2O(Na)SiPhH_3$ (Fig. 1), lies 11.8 kcal mol^{-1} above the starting reactants and contains a five-coordinated hypervalent Si center with the Ph and $PhCH_2O$ groups in equatorial and axial positions, respectively. The Na^+ cation is seemingly stabilized by both O and the Ph rings, as suggested by the close contacts between these pairs, d(Na···O) = 2.19 Å, d(Na···Ph centroid) = 2.86 and 3.54 Å.

Further stabilization of the hypervalent Si intermediate, $PhCH_2O(Na)SiPhH_3$, by the addition of BH_3 was also explored by computing the associated reaction enthalpy. Two different products are possible depending on which of the two axial faces holds BH_3. If BH_3 is introduced on the face bearing the $PhCH_2O$ substituent, the geometry optimization converges to the intermediate formulated as $PhCH_2O(Na)SiPhH_3{\cdot}BH_3$ (Fig. 1). The formation of this species is exothermic by 7.9 kcal mol^{-1} (Table 4, entry 5) and involves a Lewis acid–base interaction between BH_3 and the Ph ring attached to Si, d(B–C) = 2.01 Å. In contrast, if BH_3 is introduced on the axial face bearing the

Table 4 Reaction enthalpies in kcal mol^{-1}

Entry	Reaction	ΔH^a	$\Delta H'^b$
1	$NaBH_4 + PhCHO + SiPhH_3 \rightarrow NaBH_4 + PhCH_2OSiPhH_2$	−25.5	−25.5
2	$NaBH_4 + SiPhH_3 \rightarrow SiPhH_4Na + BH_3$	58.0	58.0
3	$NaBH_4 + PhCHO \rightarrow PhCH_2ONa + BH_3$	25.0	25.0
4[c]	$PhCH_2ONa + SiPhH_3 \rightarrow PhCH_2O(Na)SiPhH_3$	−13.2	11.8
5[c]	$PhCH_2O(Na)SiPhH_3 + BH_3 \rightarrow PhCH_2O(Na)SiPhH_3{\cdot}BH_3$	−7.9	3.9
6[c]	$PhCH_2O(Na)SiPhH_3 + BH_3 \rightarrow PhCH_2O(Na)SiPhH_2{\cdot}BH_4$	−37.3	−25.5
7	$PhCH_2O(Na)SiPhH_2{\cdot}BH_4 \rightarrow NaBH_4 + PhCH_2OSiPhH_2$	0.0	−25.5

[a] Reaction enthalpy for each reaction. [b] Reaction enthalpy with respect to initial reactants ($NaBH_4$ + PhCHO + $SiPhH_3$). [c] See Fig. 1 for a 3D-representation of the optimized geometries of $PhCH_2O(Na)SiPhH_3$, $PhCH_2O(Na)SiPhH_3{\cdot}BH_3$ and $PhCH_2O(Na)SiPhH_2{\cdot}BH_4$.

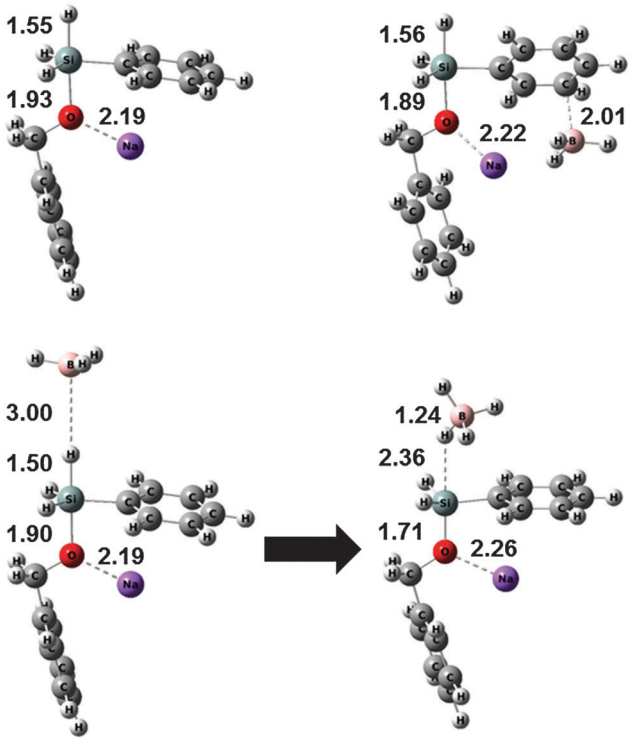

Fig. 1 Optimized structures of $PhCH_2O(Na)SiPhH_3$ (top-left) and $PhCH_2O$-$(Na)SiPhH_3{\cdot}BH_3$ (top-right). Initial (bottom-left) and final (bottom-right) structures in the geometry optimization of $PhCH_2O(Na)SiPhH_2{\cdot}BH_4$. Interatomic distances are given in Å.

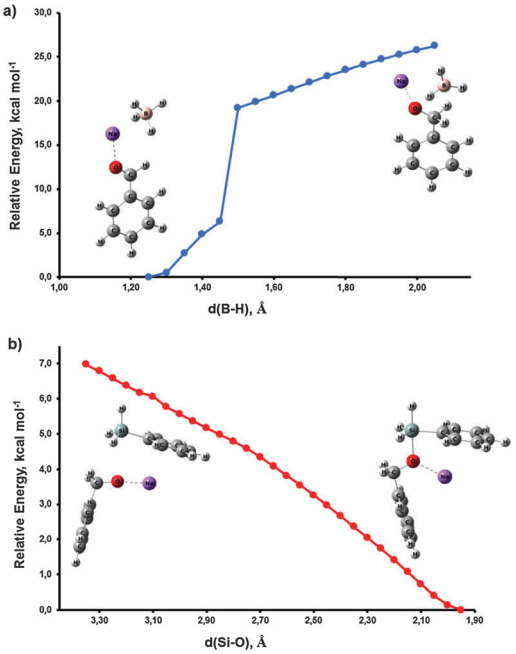

Fig. 2 Relaxed energy scans on the B–H (top) and Si–O (bottom) bonds.

hydride, the geometry optimization converges to the intermediate formulated as $PhCH_2O(Na)SiPhH_2{\cdot}BH_4$; *i.e.* BH_3 abstracts the hydride yielding the reaction product along with regenerated $NaBH_4$, d(B–H) = 1.24 Å and d(H···Si) = 2.36 Å.

Interestingly, this also happens if the geometry optimization is initiated starting from widely separated reactants, $d(BH_3{\cdots}HSi)$ = 3.00 Å. This suggests that once BH_3 transfers from the axial $PhCH_2O$-face to the opposite one, hydride abstraction occurs without any potential energy barrier. In the formation of $PhCH_2O(Na)SiPhH_2{\cdot}BH_4$, which is strongly exothermic (ΔH = −37.3 kcal mol^{-1}, Table 4, entry 6), the Si center becomes four-coordinate tetrahedral, thus losing its hypervalent character. From this intermediate, the dissociation of the final reaction product, $PhCH_2OSiPhH_2$, regenerates the catalyst, $NaBH_4$, in a thermoneutral process, ΔH = 0.0 kcal mol^{-1}. The overall reaction is exothermic by 25.5 kcal mol^{-1}.

The key steps involved in the postulated mechanism, *i.e.* hydride transfer (Table 4, entry 3) and alkoxide addition (Table 4, entry 4), were further explored computationally by focusing on their kinetics. Despite numerous attempts, the transition states of these two steps could not be located. This suggests that these reactions either proceed through extremely low and flat barriers with ill-defined transition states having very small imaginary frequencies or have no barrier on the potential energy surface. In line with this, the relaxed scans on the elongation of the B–H bond and the shortening of the Si–O bond did not yield any energy maximum (Fig. 2). Fig. 2(a) shows a steep energy increase when the B–H bond is cleaved from a distance of 1.25 Å (equilibrium distance = 1.21 Å) to 1.50 Å. From this point, the rise in energy is eased by the formation of the C–H bond. Fig. 2(b) shows a similar scenario for the formation of the Si–O bond but with the opposite energy change, which is constantly reduced as the Si–O bond is shortened from 3.35 Å to 1.95 Å (equilibrium distance = 1.93 Å). These results are consistent with $\Delta E \approx \Delta E^{\ddagger}$ in both reactions.

On the basis of this experimental and theoretical evidence we propose the potential reaction mechanism illustrated in Fig. 3. As discussed above, the reaction is initiated by reduction

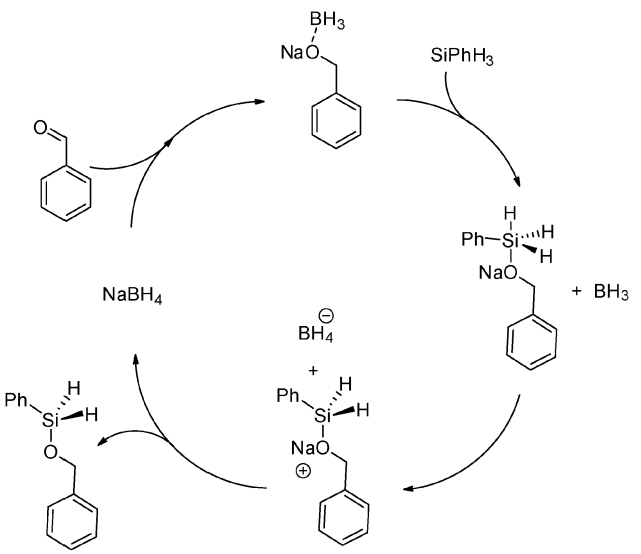

Fig. 3 Reaction mechanism postulated for the $NaBH_4$-catalysed hydrosilylation of benzaldehyde.

of the substrate at the electrophilic carbon center by the borohydride. The resulting nucleophile then attacks the silane to form a hypervalent, 5-coordinate silyl ether. Subsequent addition of BH_3 results in either the stabilization of this species or hydride abstraction, depending on which axial face of the hypervalent intermediate is involved. Hydride abstraction yields the reaction product and regenerates the catalyst.

3. Conclusions

Transition metal-free hydrosilylation of carbon–heteroatom double bonds occurs with catalytic amounts of $LiHBEt_3$ and $NaBH_4$ under mild conditions in good yields. DFT evidence suggests that hypervalent Si intermediates are involved.

4. Experimental

General

All reagents were purchased from Sigma-Aldrich, Alfa-Aesar and Fisher Chemicals and used as received unless otherwise indicated. 1-Benzoylpiperidine was synthesized by a previously reported protocol.[26] Lithium benzyloxide was synthesized by $LiBH_4$ reduction of benzaldehyde (see ESI†). All air-free reactions were run under 1 atm of dry nitrogen using standard Schlenk techniques with dried and sparged solvents. All reusable glassware and stir bars were extensively soaked in concentrated base bath to ensure a minimal risk of reaction contamination by reactive transition metals. NMR spectra were recorded at room temperature on a Bruker Avance 400 MHz NMR spectrometer running Topspin version 1.3 with a 5 mm gradient BBI probe and a BACS-60 automatic sample changer and referenced to the residual solvent peak (δ in ppm and J in Hz). GC-MS spectra recorded on Agilent 6890N GC with a 5973N MSD and a 7683 series injector using a 15 meter, 0.25 mm ID Restek Rtx-1 column.

Optimized procedure for hydrosilylation screening under N_2

To a flame dried 15 ml Schlenk tube under nitrogen was added a stir bar and 1,3,5-trimethoxybenzene (26.5 mg, internal ^{1}H NMR standard). Dried and N_2 sparged THF (4 ml) was added to the sealed Schlenk tube *via* syringe. Substrate (1.32 mmol), $LiHBEt_3$, 1 M in THF (66 μl, 0.066 mmol) and Si–H source $SiPhH_3$ (54.0 μl, 0.44 mmol–324.0 μl, 2.64 mmol) or PMHS (0.119 ml, 1.5 equivalents Si–H – 0.238 ml, 3.0 equivalents Si–H) were then added by syringe in the order listed. Elevated temperature $NaBH_4$ catalyzed reactions were prepared in the same way, with the initial addition of solid $NaBH_4$ (2.5 mg, 0.066 mmol) to the Schlenk tube instead of $LiHBEt_3$. The reaction was allowed to stir at RT −60 °C for 1–24 hours depending on the reaction. After the allotted time, the reaction was stopped by the addition of base and methanol (4 ml of 1 : 1 2 M aqueous KOH + MeOH). The reaction was allowed to stir in air for 2 additional hours at RT. Additional water was added to the solution (4 ml) and then the mixture was extracted with diethyl ether. The organic layers were collected and dried over sodium sulfate. The solvent was removed *in vacuo* and the resulting liquid was taken up in $CDCl_3$. The yield was determined by comparative integration of the product and starting material peaks to the internal standard in the ^{1}H NMR spectrum. Product identity was determined by comparing to commercially available materials.

Optimized procedure for room temperature hydrosilylation screening with $NaBH_4$ in air

To a disposable 4 dram glass vial was added a stir bar, trimethoxybenzene (56.0 mg, internal ^{1}H NMR standard) and $NaBH_4$ (5.0 mg, 0.13 mmol). THF (4 ml), $SiPhH_3$ (108 μl, 0.881 mmol) and substrate (2.64 mmol) were then added in order, as listed. The reaction was allowed to stir at RT for 1 hour. After 1 hour, the reaction was stopped by the addition 0.25 M *p*-toluenesulfonic acid in methanol (2 ml). The reaction was allowed to stir in air for 18 additional hours at RT. The solvent was then removed *in vacuo*. $CDCl_3$ (2 ml) was added to the resulting slurry and was filtered to remove insoluble excess $NaBH_4$ and silane polymer byproducts. The yield was determined by comparative integration of the product and starting material peaks to the internal standard in the ^{1}H NMR spectrum. Product identity was determined by comparing to commercially available materials.

Computational details

Structures were fully optimized without any geometry or symmetry constraints. These optimizations were done in-solvent (THF), modelled with the continuum solvation model of Truhlar and Cramer, SMD.[27] The calculations were carried out at the DFT level by using the dispersion functional of Truhlar, M06,[28] as implemented in Gaussian09.[29] The triple-ζ quality 6-311+G** basis set[30,31] was used to represent all elements. Analytic frequencies were computed in order to confirm the minimum-energy nature of all stationary points. These calculations were also used to determine the zero-point and thermal energies needed to compute the reaction enthalpies.

Acknowledgements

This research was supported by the U.S. Department of Energy (DOE), Office of Science, Basic Energy Sciences (BES), under catalysis award DE-FG02-84ER13297 (M.G.M, L.S.). We would like to acknowledge the aid of Prof. Ulrich Hintermair and Dr Jesus Campos-Manzano in advising and copy-editing this manuscript. D.B. acknowledges the Research Council of Norway for funding (Grant 179568/V30) and the Norwegian Supercomputing Program for computational resources (Grant nn4654k).

Notes and references

1 D. Addis, S. Das, K. Junge and M. Beller, *Angew. Chem., Int. Ed.*, 2011, **50**, 6004–6011.
2 S.-H. Lee, D. V. Gutsulyak and G. I. Nikonov, *Organometallics*, 2013, **32**, 4457–4464.
3 V. K. Chidara and G. Du, *Organometallics*, 2013, **32**, 5034–5037.

4 A. J. Ruddy, C. M. Kelly, S. M. Crawford, C. A. Wheaton, O. L. Sydora, B. L. Small, M. Stradiotto and L. Turculet, *Organometallics*, 2013, **32**, 5581–5588.
5 (*a*) J. Zheng, S. Chevance, C. Darcel and J.-B. Sortais, *Chem. Commun.*, 2013, **49**, 10010; (*b*) L. González-Sebastián, M. Flores-Alamo and J. J. García, *Organometallics*, 2013, **32**, 7186–7194.
6 L. Banfi, E. Narisano, R. Riva, N. Stiasni and M. Hiersemann, Sodium Borohydride, in *Encyclopedia of Reagents for Organic Synthesis*, ed. L. Paquette, J. Wiley & Sons, New York, 2004.
7 G. L. Larson and J. L. Fry, Ionic and Organometallic-Catalyzed Hydrosilane Reductions, in *Organic Reactions*, ed. S. E. Denmark, J. Wiley & Sons, New York, 2008, vol. 71.
8 (*a*) I. Cabrita and A. C. Fernandes, *Tetrahedron*, 2011, **67**, 8183–8186; (*b*) R. J. P. Corriu, J. J. E. Moreau and M. Pataud-Sat, *J. Organomet. Chem.*, 1982, **228**, 301–308; (*c*) D. V. Gutsulyak and G. I. Nikonov, *Angew. Chem., Int. Ed.*, 2010, **49**, 7553–7556; (*d*) T. Murai, T. Sakane and S. Kato, *J. Org. Chem.*, 1990, **55**, 449–453; (*e*) C. Cheng and M. Brookhart, *J. Am. Chem. Soc.*, 2012, **134**, 11304–11307; (*f*) D. Bezier, G. T. Venkanna, L. C. Misal Castro, J. Zheng, T. Roisnel, J.-B. Sortais and C. Darcel, *Adv. Synth. Catal.*, 2012, **354**, 1879–1884; (*g*) K. Junge, K. Schroder and M. Beller, *Chem. Commun.*, 2011, **47**, 4849–4859; (*h*) A. M. Tondreau, C. C. H. Atienza, K. J. Weller, S. A. Nye, K. M. Lewis, J. G. P. Delis and P. J. Chirik, *Science*, 2012, **335**, 567–570; (*i*) J. Campos, A. C. Esqueda, J. Lopez-Serrano, L. Sanchez, F. P. Cossio, A. de Coszar, E. A. Ivarez, C. Maya and E. Carmona, *J. Am. Chem. Soc.*, 2010, **132**, 16765–16767.
9 R. J. P. Corriu, R. Perz and C. Reye, *Tetrahedron*, 1983, **39**, 999–1009.
10 M. Fujita and T. Hiyama, *J. Am. Chem. Soc.*, 1984, **106**, 4629–4630.
11 M. D. Drew, N. J. Lawrence, D. Fontaine, L. Sehkri, W. Watson and S. A. Bowles, *Synlett*, 1997, 989–991.
12 C. Bornschein, S. Werkmeister, K. Junge and M. Beller, *New J. Chem.*, 2013, **37**, 2061–2065.
13 J. Fry, M. Orfanopoulo, M. G. Adlington, W. R. Dittman and S. B. Silverman, *J. Org. Chem.*, 1978, **43**, 374–375.
14 D. J. Parks and W. E. Piers, *J. Am. Chem. Soc.*, 1996, **118**, 9440–9441.
15 D. J. Parks, J. M. Blackwell and W. E. Piers, *J. Org. Chem.*, 2000, **65**, 3090–3098.
16 S. Rendler and M. Oestreich, *Angew. Chem., Int. Ed.*, 2008, **47**, 5997–6000.
17 (*a*) S. Zhou, K. Junge, D. Addis, S. Das and M. Beller, *Org. Lett.*, 2009, **11**, 2461–2464; (*b*) Y. Li, J. A. M. de La Torre, K. Grabow, U. Bentrup, K. Junge, S. Zhou, A. Bruckner and M. Beller, *Angew. Chem., Int. Ed.*, 2013, **52**, 11577–11580; (*c*) J. Fernandez-Salas, S. Manzini and S. P. Nolan, *Chem. Commun.*, 2013, **49**, 9758.
18 J. M. Blackwell, E. R. Sonmor, T. Scoccitti and W. E. Piers, *Org. Lett.*, 2000, **2**, 3921–3923.
19 K. Muther, J. Mohr and M. Oestreich, *Organometallics*, 2013, **32**, 6643–6646.
20 A. Fedorov, A. A. Toutov, N. A. Swisher and R. H. Grubbs, *Chem. Sci.*, 2013, **4**, 1640.
21 A. M. Voutchkova, D. Gnanamgari, C. E. Jakobsche, C. Butler, S. J. Miller, J. Parr and R. H. Crabtree, *J. Organomet. Chem.*, 2008, **693**, 1815–1821.
22 L. Hao, J. F. Harrod, A.-M. Lebuis, Y. Mu, R. Shu, E. Samuel and H.-G. Woo, *Angew. Chem., Int. Ed.*, 1998, **37**, 3126–3129.
23 S. Geier, P. A. Chase and D. W. Stephan, *Chem. Commun.*, 2010, **46**, 4884–4886.
24 D.-W. Wang, X.-B. Wang, D.-S. Wang, S.-M. Lu, Y.-G. Zhou and Y.-X. Li, *J. Org. Chem.*, 2009, **74**, 2780–2787.
25 F. Schubert and K. Lang, *Angew. Chem.*, 1960, **24**, 994–1000.
26 S. Zhou, K. Junge, D. Addis, S. Das and M. Beller, *Angew. Chem., Int. Ed.*, 2009, **48**, 9507–9510.
27 A. V. Marenich, C. J. Cramer and D. G. Truhlar, *J. Phys. Chem. B*, 2009, **113**, 6378–6396.
28 Y. Zhao and D. G. Truhlar, *Theor. Chem. Acc.*, 2007, **120**, 215–241.
29 M. J. Frisch, *et al.*, *Gaussian 09 (Revision. D.01)*, Gaussian, Inc., Wallingford CT, 2009.
30 R. Krishnan, J. S. Binkley, R. Seeger and J. A. Pople, *J. Chem. Phys.*, 1980, **72**, 650–654.
31 A. D. McLean and G. S. Chandler, *J. Chem. Phys.*, 1980, **72**, 5639–5648.

